Application of an iterative-perturbative inversion potential model to capture and bremsstrahlung reactions

Q. K. K. Liu
Bereich Theoretische Physik, Hahn-Meitner-Institut, D-14109 Berlin, Federal Republic of Germany

S. G. Cooper
Physics Department, The Open University, Milton Keynes, MK7 6AA United Kingdom
(Received 21 November 1994)

Two specific examples of electromagnetic transitions are used to demonstrate the ability of the macroscopic potentials determined from an iterative-perturbative inversion to reproduce the results of the microscopic resonating-group method (RGM). Phase shifts and bound state energies from a single-configuration microscopic resonating-group method calculation for ^{3}He + α have been used to construct a potential model for the ^{3}He(α,γ)^{7}Be electric-dipole capture reaction. With this potential model the astrophysical S factor at zero energy deviates from the resonating-group method result by just 3%. A potential model for the $\alpha + \alpha$ bremsstrahlung cross section, similarly constructed from $\alpha + \alpha$ resonating-group phase shifts, gives good agreement with the RGM cross section.

PACS number(s): 21.60.Gx, 25.10.+s, 25.55.Ci

Recent extensions to the iterative-perturbative (IP) method for phase shift to potential inversion allow local potentials to be determined from a selection of phase shift data as well as bound state energies [1–3]. Energy-independent potentials can now be established for a wide energy region, inclusive of the bound states, producing potentials particularly suitable for low energy reaction studies. In this work, we use calculations of electromagnetic transitions, which are often stringent tests of any nuclear models, as tools to assess the potential model. By investigating how well the results from microscopic theory can be reproduced, we hope to learn how the macroscopic potentials should be constrained to produce good agreement with the microscopic theory. Similar motivation lies behind previous comparisons of results from microscopic theory and potential model [4, 5]. Two reactions are considered as examples: the ^{3}He(α,γ)^{7}Be radiative capture and $\alpha + \alpha$ bremsstrahlung. The input into the IP method are the phase shifts and binding energies from single-configuration microscopic resonating-group method (RGM) calculations. The results based upon the potential model are compared directly with the RGM results. Given an optimum determination of the local potential, the residual disagreement in the two sets of predictions then provides an estimate of the neglected antisymmetrization effects.

The ^{3}He(α,γ)^{7}Be reaction has been thoroughly investigated by RGM [6–8] and the agreement between the best RGM results and the experimental data is quite satisfactory. Our present potential model between two-point nuclei resembles most closely the single-configuration RGM ansatz, and for more detailed comparison of wave functions we turn to the approximated RGM formalism (A-RGM), see [5] for details. It suffices to note here that the single-configuration RGM and A-RGM formalisms have identical phase shifts and bound state energies. The best RGM result is built upon successive incremental improvement of the single-configuration RGM ansatz; therefore, an accurate reproduction of the latter results is more than an academic exercise, but indicates how the IP potential might be able to account for experimental results. Further comment on this point will be given later in the text.

For the rest of this report, we shorten the cumbersome description single-configuration RGM to just RGM. The data of phase shifts and bound state energies from the RGM calculation [6] are based on a nucleon-nucleon interaction fine-tuned to reproduce the experimental bound state energies of the $\frac{3}{2}^-$ and $\frac{1}{2}^-$ states. Details of the IP inversion calculation are described in Ref. [1]. Parity dependence was introduced by using separately (a) the s- and d-wave phase shifts for the even-parity potential; (b) the p- and f-wave phase shifts, the $\frac{3}{2}^-$ and the $\frac{1}{2}^-$ bound state energies, for the odd-parity potential. Both potentials took the form

$$V(R) = V_0(R) + \mathbf{l}\cdot\mathbf{s}\, V_{so}(R). \quad (1)$$

The different geometries for $V_0(R)$ and $V_{so}(R)$ obtained for the even- and odd-parity potentials are presented in Ref. [1]. In the present study, this parity-dependent potential is labeled as IP.

The bound state energies for the $\frac{3}{2}^-$ and $\frac{1}{2}^-$ states given by potential IP agree to the second decimal place with the values from the RGM [6], -1.58 MeV and -1.15 MeV, respectively. Their radial functions are compared with the corresponding functions from A-RGM in Fig. 1. The agreement is rather close, and potential IP clearly gives functions containing the correct number of radial nodes. With these radial functions the mean square radii $\langle R^2\rangle$ given by potential IP are, respectively, 15.01 and 16.42 fm^2, compared to 14.82 and 16.38 fm^2 for the A-RGM. Very good agreement with the RGM phase shifts is obtained for $l \leq 3$ in the subthreshold energy range,

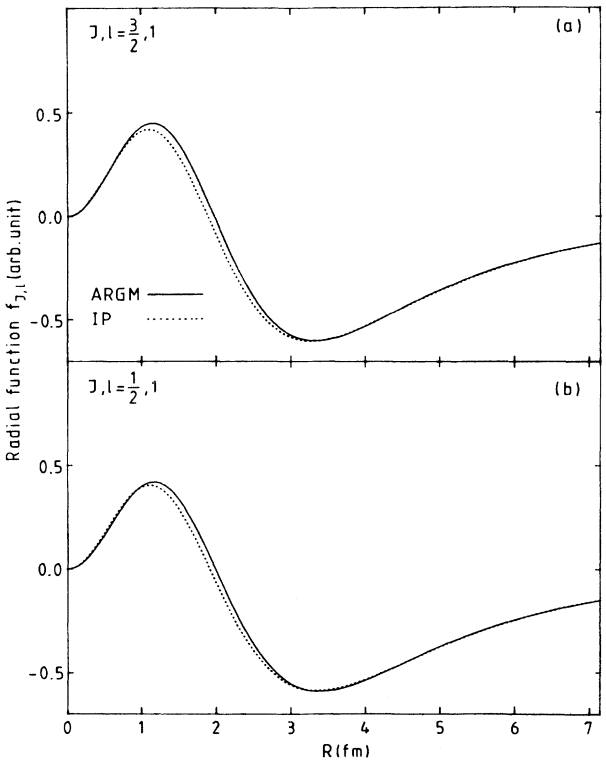

FIG. 1. Comparison of the bound state functions from A-RGM (solid line) and potential IP (dotted line). (a) $(J,l) = (\frac{3}{2},1)$. (b) $(J,l) = (\frac{1}{2},1)$.

including the f-wave resonances. Minor disagreements are noticeable only for the d-wave phase shifts. For the scattering states of $(J,l) = (\frac{1}{2},0),(\frac{3}{2},2),(\frac{5}{2},2)$, we display in Fig. 2 a comparison of s- and d-wave radial scattering functions. These are the only relevant scattering states in an $E1$ transition to the two bound states. We can conclude from the figure that the agreement for the $(J,l) = (\frac{1}{2},0)$ state is very good for $R > 3.6$ fm, and for the other two states it is for $R > 4.8$ fm. Further comment on this will be given later. Figure 2 also demonstrates that potential IP is sufficiently deep to give the radial functions of these scattering states the correct number of nodes.

The theory of radiative capture reaction in the RGM and A-RGM formalisms can be found in the literature [5, 6] and will not be repeated here. The $E1$ capture cross sections for RGM and A-RGM have been published previously. In Table I we compare them to the latest values calculated from potential IP for the summed total cross sections σ_t. The branching ratio of capture to the $\frac{3}{2}^-$ and $\frac{1}{2}^-$ states is also tabulated. We see clearly that the agreement between the results from RGM and potential IP is quite satisfactory at low energies, while the error increases to 17% at $E = 4$ MeV. The latter inaccuracy could be taken as an indication that, in this case when the nuclei overlap strongly at higher energy, a potential model may not be able to reproduce the details of the working of the Pauli principle implicit in the RGM, even though the potential-model wave functions have the same number of nodes as those from A-RGM.

As in Ref. [5], the astrophysical S factor is extracted from σ_t with the equation [7]

$$S(E) = E\ \sigma_t(E)\ \exp\left(\frac{164.514}{\sqrt{E}}\right), \tag{2}$$

with E in unit of keV. Furthermore, the energy dependence of the S factor is parametrized in the form [9]

$$S(E) = S(0)\ \exp(aE + bE^2). \tag{3}$$

In Table II, we compare the values of the S factor at zero energy $S(0)$ and the parameters a and b from RGM, A-RGM, and potential IP. The discrepancy between $S(0)$ from RGM and potential IP amounts to just 3%.

The f wave is not directly relevant to the capture cross section. However, using the f-wave phase shifts to constrain the potential helps to stabilize the inversion and consequently the capture cross section. More precisely, excluding the f-wave phase shifts from the IP inversion introduces an ambiguity problem. For example, two additional odd-parity potentials solutions have been found which reproduce both the bound state energies for the $\frac{3}{2}^-$

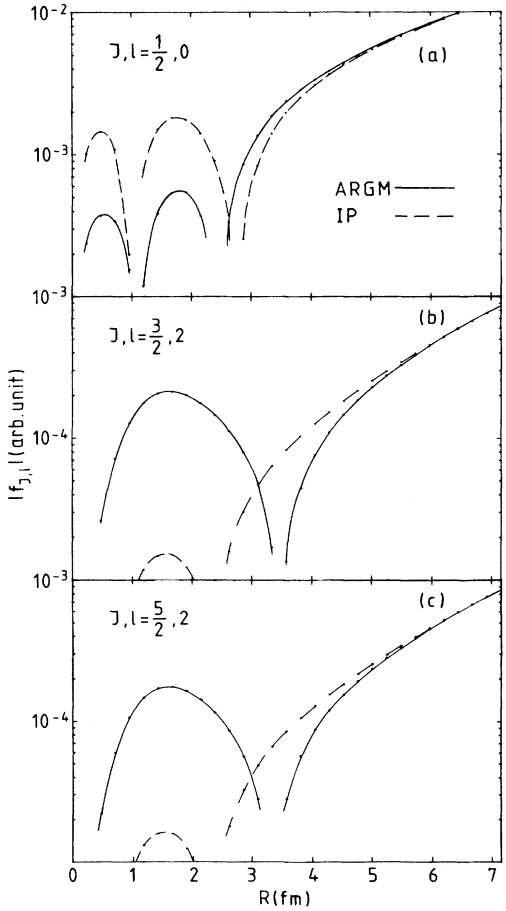

FIG. 2. Comparison of the scattering state functions from A-RGM (solid line) and potential IP (dashed line). (a) $(J,l) = (\frac{1}{2},0)$. (b) $(J,l) = (\frac{3}{2},2)$. (c) $(J,l) = (\frac{5}{2},2)$.

TABLE I. Comparison of the $E1$ capture cross sections from RGM, A-RGM, and potential IP.

	RGM		A-RGM		IP	
E (MeV)	Sum (μb)	Ratio	Sum (μb)	Ratio	Sum (μb)	Ratio
0.10	0.000473	0.414	0.000471	0.415	0.000459	0.411
0.15	0.00625	0.414	0.00624	0.415	0.00608	0.411
0.20	0.0276	0.414	0.0274	0.415	0.0268	0.411
0.50	0.658	0.417	0.654	0.418	0.642	0.415
0.75	1.496	0.422	1.487	0.423	1.451	0.420
1.70	4.381	0.438	4.335	0.439	4.042	0.439
2.06	5.363	0.441	5.296	0.442	4.858	0.443
4.00	10.159	0.442	9.892	0.444	8.453	0.450

and $\frac{1}{2}^-$ states and the p-wave phase shifts to the precision found for potential IP. These new solutions produce mean square radii of 14.57 (15.98) and 15.48 (16.9) fm^2 for the $\frac{3}{2}^-$ ($\frac{1}{2}^-$) states. The corresponding $S(0)$ obtained for these potentials are 0.6 and 0.732 keV b, to be compared to a value of 0.680 keV b obtained from potential IP.

The results above provide clear indication that the potential model from the IP inversion can accurately reproduce results from the microscopic RGM calculations for the ^{3}He(α,γ)^{7}Be electric-dipole capture reaction. Below we give a brief comparison of our analysis with other potential models in the literature [5, 10, 11].

The price for using the simpler potential model rather than a microscopic theory is that uncertainties exist in the choice of input data used to constraint the potential. As a result, different potential models for the capture reaction ^{3}He$(\alpha,\gamma)^7$Be of Refs. [10] and [11], which are claimed to have reproduced the empirical S-factor well, give results differing by nearly 10%. These investigations used potentials with parity dependence as in our present study. In [10] the potentials for the phase shifts were derived from a folding procedure, and their depths were adjusted to give the correct bound state energies and the s-wave phase shifts. In [11], the potential for the $\frac{3}{2}^-$ and $\frac{1}{2}^-$ bounds states was determined from their bound state energies and the mean square radii $\langle R^2\rangle$ of the mirror nucleus ^{7}Li. The depth of this potential was then adjusted to give the s-wave scattering length as a way to introduce parity dependence.

The IP method uses the phase shifts and the bound state energies as input data on equal footing without ad hoc readjustment. Regarding the RGM results as idealized experimental data, we have just shown that quite high accuracy can be achieved, in contrast to a previous attempt [5] which adhered to the prescription of [11].

TABLE II. Comparison of the S factors at zero energy $S(0)$ and the parameters a and b from RGM, A-RGM, and potential IP.

	$S(0)$ (keV b)	a	b
RGM	0.702	−0.597	−0.0652
A-RGM	0.700	−0.601	−0.0636
IP	0.680	−0.567	−0.0976

There the exact agreement with the RGM s-wave scattering length was obtained at the expense of total disagreement in the d-wave phase shift. We have in effect opted for constraints different from [11] to impose on the potentials. For the even-parity potential, we have opted for a much better fit of the d-wave phase shifts as opposed to reproducing the s-wave scattering length, i.e., we now obtain 19.8 fm for the s-wave scattering length, to be compared with 28.2 fm from RGM. For the odd-parity potential, we have obtained a better fit to the $\frac{5}{2}^-$ and $\frac{7}{2}^-$ resonances in place of accurately fitting the mean square radii of the $\frac{3}{2}^-$ and $\frac{1}{2}^-$ bound states. The resultant $S(0)$ deviates from the RGM value by only 3%, an improvement over the previous discrepancy [5] of 7.5%. Our result supports the suggestion of [4] that simultaneous fitting of the bound state energies and phase shifts by a potential model is important for the agreement between a potential model and microscopic cluster theory.

In a general context, a potential model is never expected to be able to reproduce all facets of a microscopic theory. High accuracy in some quantities might be achieved at the expense of the obverse in others. This affects the constraints one chooses to impose on the local potential. For this capture reaction, we may conclude that the macroscopic potential should be determined from the $\frac{3}{2}^-$ and $\frac{1}{2}^-$ bound state energies simultaneously with the $l = 0, 1, 2, 3$ phase shifts, rather than the mean square radii and the scattering length. An examination of the wave functions for the potential model in Ref. [5] reveals that, in adjusting that potential to reproduce the mean square radii, errors were introduced into the wave function normalization in the asymptotic region. This error translates to an error in the capture cross section of 8%. We have also tested the condition related to the s-wave scattering length by renormalizing the even-parity potential to reproduce exactly the value 28.2 fm^2 for it. The $S(0)$ becomes 0.631 keV b, which is in worse agreement with the RGM value.

If the capture reaction is entirely from the exterior region, then the hard-core model would have sufficed. This was disproven in [5], where it was established that for capture below the Coulomb barrier, even at zero energy, the region inside the barrier to as low as $R = 3.6$ fm, i.e., some way inside the barrier, also contributes, although the main contribution does come from outside the bar-

rier. We examine below a second type of electromagnetic transition and show further evidence that the extended IP potential model also gives good agreement with RGM results when contributions from inside the barrier become more important.

We have made calculations of the $\alpha+\alpha$ bremsstrahlung cross section based on IP inversion of the $\alpha + \alpha$ RGM (single-configuration) phase shifts [12]. We have determined a local potential which is a noticeable improvement upon the deep potential of Ref. [13] for energies up to 16 MeV and $l \leq 6$. In fact, the IP potential produces curves for the phase shifts which go through all the RGM data points in Fig. 1 of [12]. The bremsstrahlung cross section is calculated for the detection angles $\theta_A = \theta_B = 27°$, such that the $E2$ transition takes place between the $l = 4$ resonance at 12.1 MeV and the $l = 2$ resonance at 2.9 MeV. In this resonance to resonance transition, the wave functions from the IP potential are being tested for its ability to reproduce the RGM results with important contribution from inside the barrier. The RGM and potential model cross sections are shown in Fig. 3. Clearly the potential model gives a satisfactory account of the RGM values, although further effects due to antisymmetrization are not completely negligible.

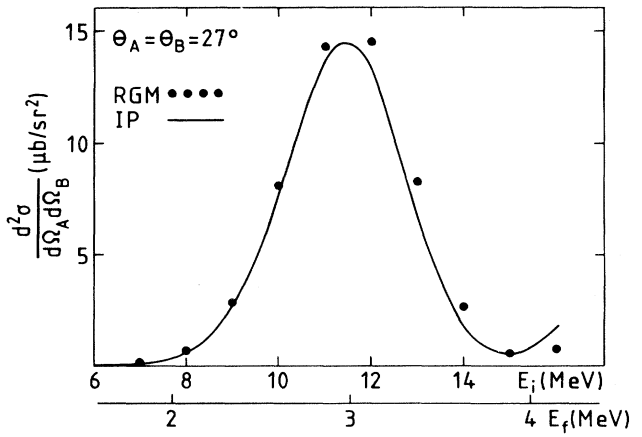

FIG. 3. The double cross section $d^2\sigma/d\Omega_A d\Omega_B$ (μb/sr^2) as a function of the incident energy E_i for polar detection angles $\theta_{A,B} = 27°$. A scale for the final energy E_f is included. The results of RGM are denoted by solid dots and potential IP by a solid line.

Due to the good agreement between the results from RGM and the IP potential, we are encouraged to speculate how the methods used above could be used to analyze real empirical data. That is, empirical phase shifts and bound state energies could be used as input data for the IP potential, while, at the same time the capture cross section ought to be multiplied by the spectroscopic factor for the ^{3}He + α clustering in the $\frac{3}{2}^-$ and $\frac{1}{2}^-$ bound states [14]. We suggest that the present case might be used to provide guidelines for choosing a potential in cases where microscopic calculations are difficult to obtain. The $E2$ transition in the ^{12}C$(\alpha,\gamma)^{16}$O capture reaction is a possible example, since the relevant bound states and partial waves could be approximated quite well from a ^{12}C + α clustering point of view [15] and local $\alpha+^{12}$C potentials have already been established from empirical phase shifts [16].

We have presented two specific examples of electromagnetic transitions, illustrating the accuracy to which a fully microscopic model can be reproduced by a simple potential model. In particular, we have shown that by using potentials determined by IP inversion to reproduce a range of phase shifts and bound state energies very accurately, a value of the zero-energy S factor $S(0)$ for the ^{3}He$(\alpha,\gamma)^7$Be reaction is obtained which deviates from the RGM results by 3% only.

[1] S. G. Cooper, Phys. Rev. C **50**, 359 (1994).
[2] S. G. Cooper and R. S. Mackintosh, Phys. Rev. C **43**, 1001 (1991).
[3] S. G. Cooper, R. S. Mackintosh, A. Csoto, and R. G. Lovas, Phys. Rev. C **50**, 1308 (1994).
[4] D. Baye and P. Descouvemont, Ann. Phys. (N.Y.) **165**, 115 (1985).
[5] Q. K. K. Liu, H. Kanada, and Y. C. Tang, Phys. Rev. C **33**, 1561 (1986).
[6] Q. K. K. Liu, H. Kanada, and Y. C. Tang, Phys. Rev. C **23**, 645 (1981).
[7] H. Walliser, Q. K. K. Liu, H. Kanada, and Y. C. Tang, Phys. Rev. C **28**, 57 (1983); H. Walliser, H. Kanada, and Y. C. Tang, Nucl. Phys. **A419**, 133 (1984).
[8] T. Kajino and A. Arima, Phys. Rev. Lett. **52**, 739 (1984).
[9] R. D. Williams and S. E. Koonin, Phys. Rev. C **23**, 2773 (1981).
[10] P. Mohr, H. Abele, R. Zweibel, G. Staudt, H. Krauss, H. Oberhummer, A. Denker, J. W. Hammer, and G. Wolf, Phys. Rev. C **48**, 1420 (1993).
[11] B. Buck, R. A. Baldock, and J. A. Rubio, J. Phys. G **11**, L1 (1985).
[12] Q. K. K. Liu, Y. C. Tang, and H. Kanada, Few-Body Systems **12**, 175 (1992).
[13] Q. K. K. Liu, Nucl. Phys. **A550**, 263 (1992).
[14] H. Walliser and Y. C. Tang, Phys. Lett. **135B**, 344 (1984).
[15] P. Descouvemont, D. Baye, and P.-H. Heenen, Nucl. Phys. **A430**, 426 (1984); P. Descouvemont and D. Baye, Phys. Rev. C **36**, 1249 (1987); P. Descouvemont, *ibid.* **47**, 210 (1993).
[16] S. G. Cooper and R. S. Mackintosh, Nucl. Phys. **A517**, 285 (1990).